Journal of Research in Pharmacy

Research Article

www.jrespharm.com

Formulation and optimization of Agomelatine loaded nanostructured lipid carriers for intranasal delivery

Shailendra SALVANKAR [1] *, Komal THITE [1], Mukesh RATNAPARKHI [1], Gajanan KULKARNI [1]

[1] Department of Pharmaceutics, Marathwada Mitra Mandal's College of Pharmacy, Pune-411033, India.
* Corresponding Author. E-mail: salvankar@gmail.com (S.S.); Tel. +91-942-320 98 75.

Received: 30 August 2023 / Revised: 26 December 2023/ Accepted: 28 December 2023

ABSTRACT: The current study aims to prepare agomelatine-loaded nanostructured lipid carriers (AGO-loaded NLCs) and their administration through the intranasal route in an attempt to circumvent hepatic metabolism, facilitate controlled release, and increase cerebral distribution, etc. Agomelatine faces several challenges such as a fast metabolic process, limited solubility, gastrointestinal vulnerability, enzymatic cleavage, and decreased bioavailability. These challenges collectively undermine its therapeutic effectiveness. Therefore, the goal of the current work is to develop agomelatine-loaded NLCs with enhanced drug entrapment, extended release, and improved stability. Agomelatine-loaded NLCs were prepared by using Glyceryl monostearate and Neroli oil as solid lipid and liquid lipid respectively, While Tween 80 and poloxamer 188 were used as surfactant and co-surfactant. The technique of melt emulsification ultrasonication was employed to prepare these NLCs. The prepared formulation was optimized utilizing a three-factor, three-level Box-Behnken design with total lipid percentage, surfactant, and co-surfactant percentage, and ultrasonication time as independent variables and particle size, zeta potential, and percentage entrapment efficiency as dependent variables. The optimized NLCs size was found to be 122 ± 3.19 nm and the results from transmission electron microscopy are likewise within this size range (under 150 nm) and showed that the particles were homogeneous and nearly spherical, with porous and irregular surface features. Polydispersity index, zeta potential, entrapment efficiency, and drug release % were observed as 0.353 ± 0.15, -33.7 ± 2.35 mV, 90.57 ± 0.984% and 94.65 ± 2.39% respectively. The findings from the permeation study indicated a substantial enhancement in permeation for AGO-loaded NLCs when compared to AGO solution.

KEYWORDS: Agomelatine; Blood brain barrier; Box-Behnken design; Intranasal delivery; Nanostructured lipid carriers.

1. INTRODUCTION

According to the survey of Global Burden of Disease for 2019, the sixth most prevalent ailment affecting persons between the ages of 10 to 24 years is depression and it also exists behind most of the suicidal tendencies [1]. Depression is a condition that impairs cognitive functions, expands sensitivity to somatic symptoms, and has an impact on ordinary life [2]. The initial onset of depression typically occurs when a person begins to lose interest, develops insomnia, feels apprehensive, or reduces confidence. The most serious problem associated with it is that chronic depression can progress into severe depressive disorder which impacts a person's social and economic life. Currently available antidepressants such as fluoxetine, escitalopram, and citalopram which comes under the class of selected serotonin reuptake inhibitors (SSRIs) have been commonly used for treating depression. But due to these SSRIs, the patients are suffering from a number of side effects, including weight gain, drowsiness, trembling, and sexual dysfunction [3,4]. Hence, the selection of the potential antidepressant drug is needed which will avoid these side effects and in turn enhance the effectiveness of the drug and patient compliance during therapy [5].

A new antidepressant drug agomelatine (AGO) has shown potential and clinical outcomes in addressing the symptoms of depression [6-8]. Agomelatine has melatonin agonistic activity on M1 and M2 receptors due to which it shows milder side effects than other currently licensed antidepressant drugs by controlling circadian rhythms and restoring sleep cycle [9-12]. Even though AGO has adequate antidepressant efficacy it shows little adverse effects (like sexual dysfunction, weight gain, etc.). It is less commonly used for oral administration due to its limited solubility as well as rapid first-pass metabolism (oral bioavailability <5%, half-life 1–1.5 hours). Hence, the other effective route of administration is required

How to cite this article: Salvankar S, Thite K, Ratnaparkhi M, Kulkarni G. Formulation and Optimization of Agomelatine loaded Nanostructured Lipid Carriers for Intranasal Delivery. J Res Pharm. 2024; 28(5): 1592-1608.

ISSN: 2630-6344

http://dx.doi.org/10.29228/jrp.837

to address these challenges associated with the oral administration of AGO. Therefore, several administration routes were examined from which the intranasal route was found to be suitable as it can alleviate the issues related to oral administration. Intranasal drug delivery also circumvents the several levels of the human brain such as the cerebral spinal fluid (CSF) and the blood-brain barrier (BBB) which limits the potency and efficiency of drug that enters the brain [13]. The nasal route enhances the availability of the drug owing to its huge, deeply vascularized surface area and the impassable diversions provided by the BBB [14-17]. Nasal drug delivery devices have recently attracted a lot of attention as it is a non-invasive method for delivering drugs directly into the brain via the trigeminal neuronal region and the olfactory region of the nasal epithelium for diameters less than 200 nm [18]. Additionally, intranasal administration of drugs offers benefits, like avoidance of gastrointestinal enzyme degradation, hepatic first-pass metabolism, and reduced plasma protein binding which results in the enhancement of therapeutic impact and increased drug availability at the site of action. Recently intranasal delivery systems built on nanosystems have received a lot of attention because of nanosystems excellent biocompatibility, the capacity to keep lipophilic compounds solubilized, and improved stability. Lipid-based nanosystems, such as lipid nanoparticles, liposomes, nanoemulsions, and microemulsions, have shown successful outcomes in increasing drug bioavailability [19-24]. One of the forms i.e. Nanostructured lipid carrier (NLC) which is an innovative and advanced lipid colloidal system with benefits like a substantial drug-carrying capacity, improved structural integrity, increased accessibility, and regulated drug release [25-27]. It is primarily made up of a binary lipid mixture and furthermore, the surfactant system stabilizes it by interacting with the surrounding water phase. The binary lipid combination consists of a solid lipid and a liquid lipid, and these two lipids work together to generate a matrix system that prevents the solid lipid from recrystallizing and also promotes thermodynamic stability [28]. As the lipid component of nanostructured lipid carriers (NLCs) makes it easier for drugs to pass through the stratum corneum, they can be employed as a successful strategy to increase drug penetration through the skin layers [29]. In this work, an attempt has been made to develop the agomelatine-loaded nanostructured lipid carriers (AGO-loaded NLCs) using neroli oil as a liquid lipid for the first time in the intranasal delivery of the drug. Neroli oil is obtained through steam distillation from the aromatic blossoms of the Citrus aurantium tree, commonly known as the orange tree. This essential oil has demonstrated advantages in both skincare and emotional well-being. Its applications encompass alleviating sensations of depression and sorrow, countering feelings of loss, promoting serenity, and fostering a sense of joy.

2. RESULTS AND DISCUSSION

2.1. Screening of Solid lipid and Liquid lipid

Among the five solid lipids i.e., Glyceryl monostearate (GMS), Stearic acid, Compritol 888ATO, Precirol ATO 5, and Gelucire 43/01 screened for solubility study with AGO, from which the GMS showed maximum solubility of AGO as shown in Table 1. GMS is saturated monoglycerides and saturated monoglycerides exhibit enhanced capability to initiate fat crystallization and superior emulsification potential in comparison to unsaturated monoglycerides. GMS has a long chain of fatty acids with eighteen carbon atoms, and as the chain length of fatty acids increases, there is a corresponding rise in the melting point, leading to a progressive transformation in physical state, transitioning from a liquid oil to a solid fat, and eventually into a solid waxy form. Besides that the hydrophilic properties are inversely proportional to the number of carbon atoms of fatty acids and as we know that GMS has a higher number of carbon atoms it can show weak hydrophilic properties. However, GMS can show strong lipophilic properties which would help in the permeation of molecules into a biological membrane due to their lipophilic nature [30]. Hence, amongst selected solid lipids, GMS was finalized for the preparation of NLCs.

Among the selected liquid lipids, Castor oil, Oleic acid, Mono & diglycerides, and Neroli oil were natural oils and Isopropyl myristate was synthetic oil. All of these were screened for solubility study with AGO and the results were provided in the Table 1. In which the AGO showed maximum solubility in the neroli oil as compared to other liquid lipids. Neroli oil is an essential oil and essential oils have no specific cellular ligands due to their complex chemical composition. After conjugating with the drug they become lipophilic mixtures, which are easily able to cross the cell membranes by degrading the layers of polysaccharides, phospholipids, and fatty acids. Hence, Neroli oil was finalized for further formulation of NLCs. Chosen lipids showed the requisite stability and were confirmed to be safe with the mucus layer and several cell types [31, 32].

Table 1. Solubility results of Agomelatine in various solid and liquid lipids

Screening of Lipids		Solubility of Agomelatine (mg/ml)
Solid Lipids	GMS	81 ± 1.9
	Stearic acid	66 ± 0.917
	Compritol 888ATO	63 ± 1.523
	Precirol ATO 5	59 ± 0.651
	Gelucire 43/01	47 ± 0.771
Liquid Lipids	Neroli oil	40.42 ± 1.042
	Mono & diglyceride	32.11 ± 0.884
	Oleic Acid	33.03 ± 1.32
	Iso-propyl myristate	12.18 ± 0.976
	Castor oil	15.77 ± 0.531

Each value represents mean ± SD (n=3)

2.2. Selection of surfactant and co-surfactant for the preparation of NLC

The selection of surfactant and co-surfactant was done by analyzing the transmittance % of formulation using the surfactants (Table 2). Accordingly, Tween 80 was selected as a surfactant to produce NLC. Tween 80 has a longer aliphatic tail which results in a more lipophilic nature. Polysorbate 80 (Tween® 80), a non-ionic surfactant consists of a polyoxyethylene chain that encompasses a tetrahydrofuran ring, and the presence of this unique structure serves the essential purpose of steric stabilization. Increasing the length of the non-polar chain has been observed to positively correlate with an increase in solubility. This phenomenon can be attributed to the hydrophobic tail's role in preventing particle aggregation. Its selection was confirmed by prior research, which demonstrated its compatibility with the employed lipids. Poloxamer 188 is more hydrophilic than Poloxamer 407. Therefore, Poloxamer 188 was selected as a co-surfactant due to its capability to emulsify selected $lipid_{mix}$, its gentle impact on the nasal mucosa without causing irritation, and its tendency to reduce the polymorphic state transitions of lipids.

Table 2. Transmittance shown by different surfactant solutions after dissolving the binary lipid

Surfactant & Co-surfactant	Transmittance % ± SD
Span 20	55.60 ± 0.9
Span 80	65.10 ± 0.6
Tween 20	80.30 ± 0.3
Tween 40	83.80 ± 1.3
Tween 60	87.90 ± 2.1
Tween 80	91.62 ± 2.5
Poloxamer 407	89.15 ± 1.2
Poloxamer 188	94.60 ± 2.8

Each value represents mean ± SD (n=3)

2.3. Characterization of AGO-loaded NLCs

2.3.1. Fourier transform infrared spectroscopy (FTIR) study

The FTIR spectra's of active pharmaceutical ingredient (API) AGO, drug with GMS, drug with liquid lipid (Neroli oil), and drug with surfactant & co-surfactant are shown in Figure 1. Figure 1(A) shows the FTIR spectra of API AGO, which showed all the characteristic peaks of AGO. The peak observed at 1249 cm^{-1} represents alkyl ketone. A peak at 1644.68 cm^{-1} and 1732.67 cm^{-1} represented C=C (alkene group) and C=O (carbonyl group), respectively. The peak at 3392.80 cm^{-1} shows –NH group. Characteristics peaks of the GMS can be seen in Figure 1(B) at around 3321.42 cm^{-1} OH group and peak at 2922 cm^{-1} represented C–H group. While a peak at 1462.04 cm^{-1} is indicative of the C–H_3 group. Also, the peaks obtained at 1249 cm^{-1} and 3375 cm^{-1} were found to be similar with alkyl ketone and –NH group of API AGO. In Figure 1(C) peaks of Neroli oil can be seen at 1440.83 cm^{-1} CH_3 group, CH_2 group at 2968.45 cm^{-1}, and NH group at 3396.64 cm^{-1}. In Figure 1(D) surfactant and co-surfactant (Tween 80 and poloxamer 188) characteristic peaks were observed at 1651.07 cm^{-1} depicting the carbonyl group and OH group showing at 3419.79 cm^{-1}. Also, CH_2 and CH_3

showed a range at 2927.94 cm^{-1} and 2941.44 cm^{-1} respectively. According to this obtained data, it can be assumed that there was less possibility of interaction between the drug and the other excipients as no any significant changes were observed in the characteristic peaks of AGO when combined with the above-mentioned excipients.

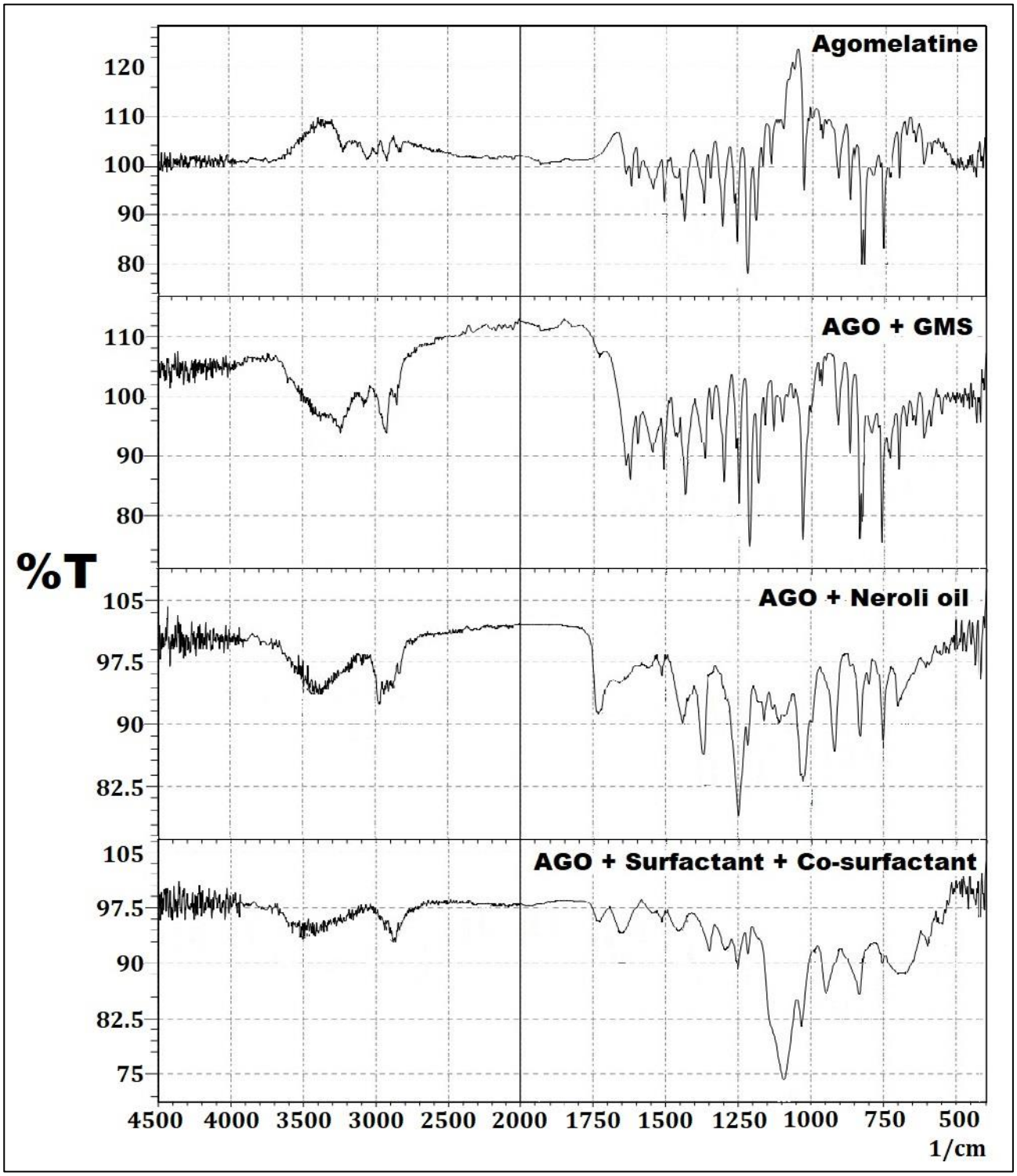

Figure 1. FTIR spectra of A) API Agomelatine B) AGO+GMS C) AGO+Neroli oil D) AGO+Surfactant+Co-surfactant

2.3.2. Differential scanning calorimetry (DSC) study

AGO shows a sharp endothermic peak at 110°C that depicts its crystalline nature. In the thermogram of an optimized batch of NLC, the disappearance of the peak depicts that shift in the thermal characteristics of AGO. This alteration could be attributed to the thorough integration or complete dissolution of the drug molecules within the lipid phase. The disappearance of the AGO peak further corroborates the earlier observation regarding the drug's solubility within GMS, affirming its complete and increased encapsulation within the nanocarriers system. In conclusion, we can say that the oil and excipients masked the drug and changed its nature from crystalline to amorphous form which will be useful for the enhancement of solubility (Figure 2) [33].

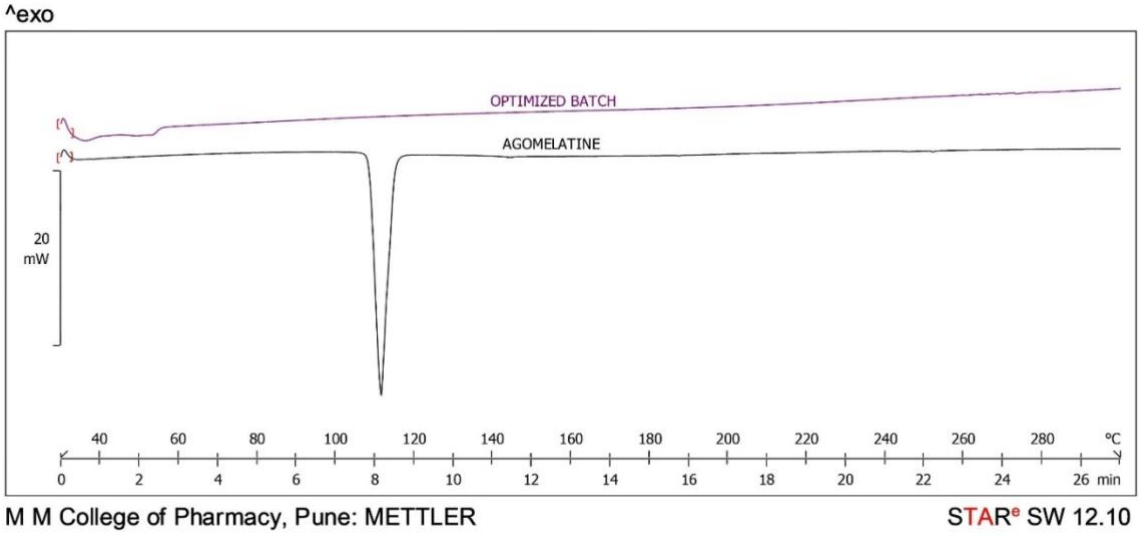

Figure 2. DSC thermogram of Agomelatine and Optimized batch of AGO-loaded NLCs

2.3.3. Entrapment efficiency %

The percent entrapment of drug for the prepared batches of AGO-loaded NLCs is presented in Table 3. The entrapment efficiencies ranged between 60.31 to 91.91%. The observed findings show that as the lipid concentration increases there is a corresponding rise in entrapment efficiencies. This may occur due to the fact that elevated lipid concentration leads to the formation of larger particles which could have a significant impact on the effectiveness of entrapping the drug that resides on the surface.

2.3.4. Data analysis and formulation optimization

The particle size of prepared AGO-loaded NLCs was found in between 111 to 198 nm. The zeta potential ranged from -20 mV to -46 mV which is in the suitable range for the stabilization of formulation. The Box-Behnken design with three levels and three factors was utilized for the process of optimization. The Quadratic polynomial models were determined to be the specific model terms that best account for all three factors. The model terms indicated that independent factors directly affected dependent variables (responses). The optimized experimental parameters were determined by comparing all of the observed responses. The 13 runs of experimental design with their corresponding responses are displayed in Table 4. All of the 3D response surface plots are shown in Figure 3 demonstrating the influence of different factors on the responses.

Effect of independent factors on response 1 (Particle size)

According to the obtained results, particle sizes of all the developed formulations vary between 111 nm to 198 nm. More thorough information about the impact of numerous independent parameters on particle size is provided by a 3D response surface graph (Figure 3). The response showed a clear relationship between the concentration of total lipid and the size of the NLC formulation. The outcome revealed that particle size increased as the total lipid percentage increased. Additionally, the size of NLC is substantially

influenced by surfactant concentration. The quadratic model, which was recommended earlier shown to be a significant model with an F value of 14.17 and an R^2 value of 0.9770 (Table 5).

Table 3. Entrapment efficiency % of AGO-loaded NLCs

Batch	EE (%)
1	80.74 ± 0.403
2	80.05 ± 0.135
3	91.91 ± 1.183
4	71.32 ± 1.971
5	79.14 ± 0.215
6	68.41 ± 1.147
7	60.31 ± 2.009
8	65.94 ± 0.475
9	88.93 ± 0.385
10	65.93 ± 2.008
11	87.85±0.343
12	65.94±0.560
13	67.89±2.158

Each value represents mean ± SD (n=3)

Table 4. Effect of various formulation variables (independent factors) on the characteristic features of the NLCs prepared using Box-Behnken design for optimization of the formulation

Sr. No.	Run	Factor 1 A: Total Lipid %	Factor 2 B: Surfactant	Factor 3 C: Sonication Time	Response 1 Particle Size (nm)	Response 2 Zeta Potential (mV)	Response 3 EE %
1	1	2.5	2	5	141	-33	80.74
2	2	1	1.5	10	145	-46	80.05
3	3	2.5	1.5	7.5	122	-33	91.91
4	4	2.5	2	10	148	-32	71.32
5	5	2.5	1	10	170	-20	79.14
6	6	4	1.5	5	116	-46	68.41
7	7	2.5	1	5	148	-24	60.31
8	8	1	2	7.5	147	-20	65.94
9	9	4	1.5	10	170	-33	88.93
10	10	1	1	7.5	111	-32	65.93
11	11	1	1.5	5	198	-24	87.85
12	12	4	2	7.5	132	-46	65.94
13	13	4	1	7.5	146	-20	67.89

Table 5. Model fitting of responses and analysis of variance (ANOVA)

Response	Model fitting	R^2	Adjusted R^2	SD	% CV
Particle Size	Quadratic	0.9770	0.9081	13.13	8.12
Zeta potential	Quadratic	0.9717	0.8867	3.30	10.44
Entrapment efficiency	Quadratic	0.9636	0.8542	3.95	5.31

There will be only a 2.58% chance that noise would result in an F-value this large. P-values found to be less than 0.05 indicating that model terms were significant and in this case, A, B, AC, A^2, and C^2 were significant model terms (Eq. 1).

$PS = 122 + 25.36 * A + 18.86 * B + 11.5 * C + 8.025 * AB + 34.25 * AC - 0.75 * BC + 42.7625 * A^2 - 10.24 * B^2 + 31.99 * C^2$ …….. (1)

Effect of independent factors on response 2 (Zeta potential)

The quadratic model, which was recommended earlier shown to be a significant model with an F value of 11.44, P-value < 0.05 and an R^2 value of 0.9717 (Table 5). It was just by accident that noise caused 3.48% of the "model F value" to be this large. B, AB, and AC are important model terms in this situation (Eq. 2). The zeta potential decreased towards a more negative value when the surfactant concentration and the total lipid percentage were increased, as observed in Figure 3.

$ZP = -33.51 - 2.87 * A - 4.47 * B - 0.5937 * C - 9.5 * AB + 8.75 * AC - 0.9375 * BC - 2.90 * A^2 + 6.91125 * B^2 - 0.8387 * C^2$ …….. (2)

Effect of independent factors on response 3 (Entrapment Efficiency %)

On the basis of the response plot (Figure 3), it can be depicted that the optimum percentage of total lipid and surfactant have resulted into the greater entrapment of drug inside the developed NLCs. Although the quadratic model, which was recommended earlier found to be a significant model with an F value of 8.81, P-value < 0.05 and an R^2 value of 0.9636 (Table 5). And there was only a 5.00% probability that noise would result in a "model F value" this large. The important model terms in this instance are AC, BC, A^2, and B^2 (Eq. 3).

$EE = 91 - 1.125 * A + 1.25 * B + 2.875 * C - 0.5 * AB + 6.75 * AC - 7 * BC - 8.625 * A^2 - 16.875 * B^2 - 1.625 * C^2$ …….. (3)

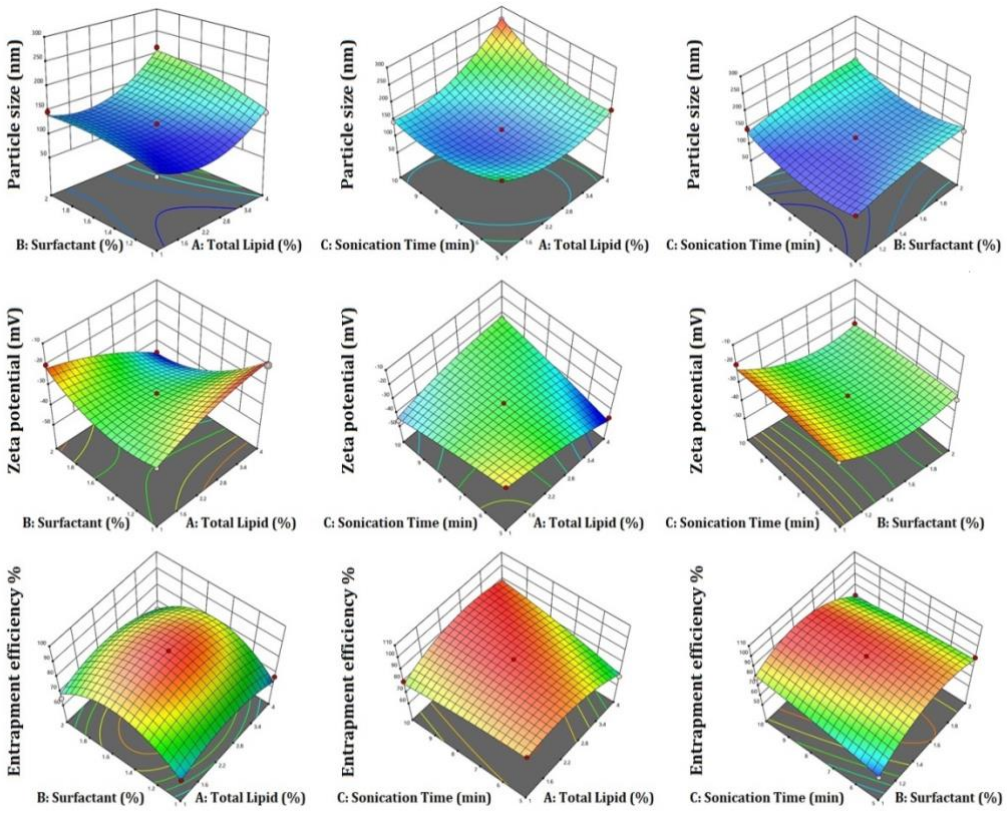

Figure 3. 3D surface plot showing effect of independent variables on particle size, zeta potential & entrapment efficiency % of AGO-loaded NLCs formulations

2.3.5. Optimization and point prediction

The optimized values for parameters were obtained by following the statistical analysis and assessment of the effects of different parameters on the responses. The optimization process yields precise formulation parameters to achieve the intended objectives of the proposed work. The statistical optimization using the Box-Behnken design recommended that the formulation variables should be configured to 2.5% Total Lipid, 1.5% Surfactant Concentration, and 7.5 minutes of Ultrasonication Time as the most favorable values to obtain minimum particle size and maximum zeta potential and entrapment efficiency. The

predicted outcomes for the optimized formulation, as determined by DesignExpert® were observed as 122 nm, -33 mV, and 91 % for particle size, zeta, and entrapment efficiency correspondingly. The final optimized batch was prepared employing the suggested proportions, followed by subsequent evaluation procedures.

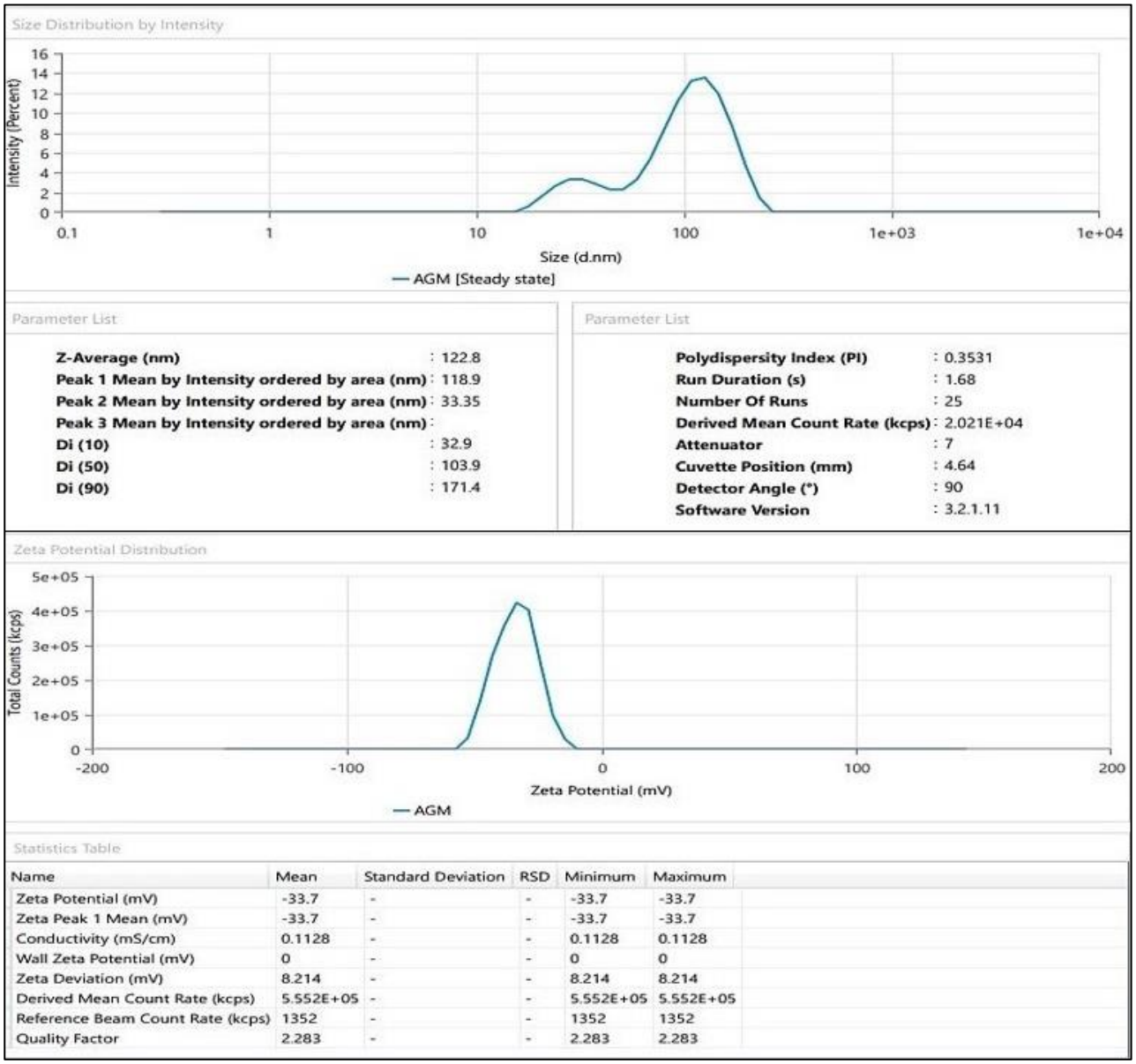

Figure 4. Particle Size & Polydispersity index and Zeta potential graph of optimized batch

2.3.6. Particle size, Polydispersity index (PDI), zeta potential, and entrapment efficiency %

According to design optimization, the final batch was prepared and subjected to analysis for particle size, polydispersity index (PDI), zeta potential, and entrapment efficiency. The observed particle size was 122 ± 3.19 nm, PDI 0.353 ± 0.15, and zeta potential – 33.7 ± 2.35 mV (Figure 4). Moreover, the entrapment efficiency of optimized AGO-loaded NLCs was found to be 90.57 ± 0.984 %. The statistical design software predicted values for the optimized NLC and obtained values of the particle size, zeta potential and entrapment efficiency were extremely similar. The almost monodispersed particles and narrow size distribution were revealed by the PDI of 0.353 for pharmaceutical nanoparticulate systems. The ideal value of PDI should be less than 0.5, and the majority of previously reported NLC studies fall within this range. The charge on the nanocarrier's surface is examined using the zeta potential, which also serves to forecast the stability of the nanocarriers because the stability increases as the electrostatic attraction among the particles increases. The optimized AGO-loaded NLC was noted with a zeta potential of – 33.7 ± 2.35 mV from which it can be inferred that the dispersal has good physical stability which prevents aggregation with aging.

Additionally, the negative charge on the produced NLCs surface was determined to be acceptable for human use and appropriate for intranasal use [16].

2.3.7. Transmission Electron Microscopy (TEM)

Transmission electron microscopy (TEM) investigation provided visible confirmation of the optimized AGO-loaded NLC. Figure 5 shows that NLC images have homogeneous shapes and do not adhere to one another. Additionally, TEM photomicrographs indicated that NLC particles had a diameter under 150 nm, which was consistent with the average hydrodynamic diameter as previously described and determined using the dynamic light scattering (DLS) technique.

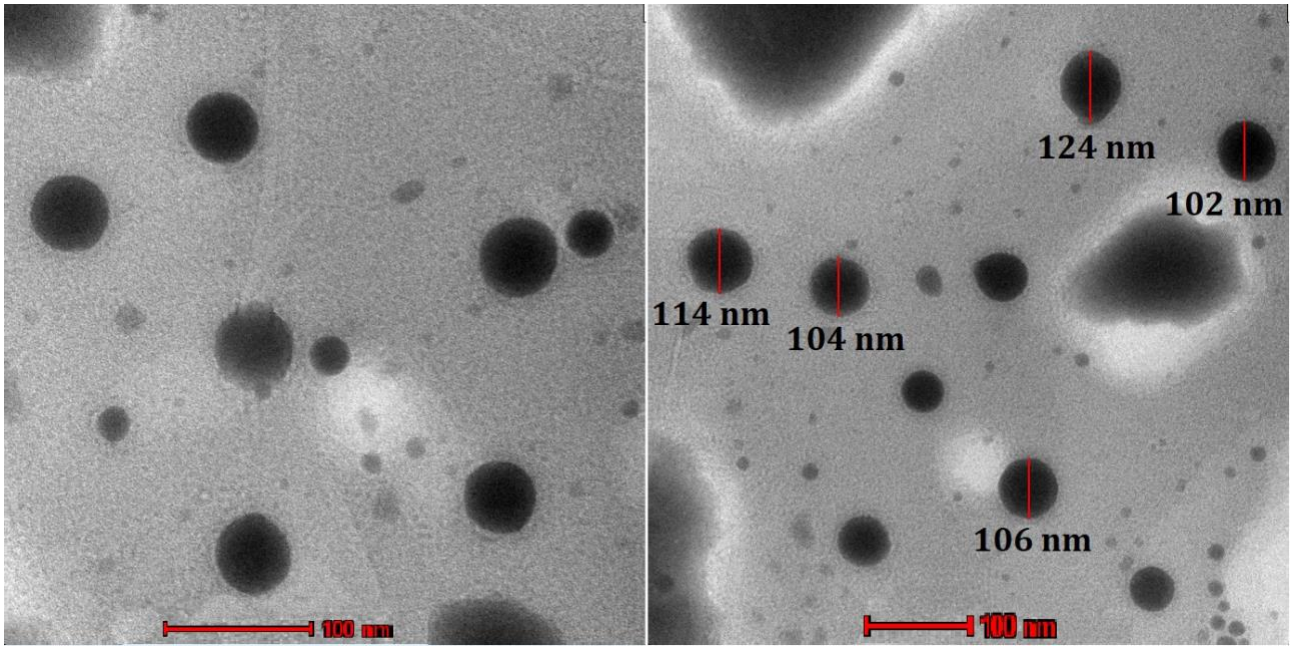

Figure 5. Transmission electron microscopy images of optimized AGO-loaded NLCs batch

2.3.8. In-vitro drug release study

The Franz diffusion cell device was used in the in-vitro drug release tests, together with a dialysis membrane and Phosphate buffer solution (PBS) 6.8. The drug release profiles of all formulated batches of AGO-loaded NLCs showed good release profiles. More than 90% of AGO in F1, F2, F3, F4, F5, F7, F10, F11 and F12 was released and dissolved within 300 min, while 80-90% AGO in F6, F8, F9 and F13 was released in 300 min. Furthermore, the drug release characteristics of the optimized batch of AGO-NLC and AGO solution were compared (Figure 6). AGO-NLC showed continuous drug release, which corroborated that the sustained delivery of the intended drug and, by extension, the efficacy of the produced formulation can be enhanced. On the other hand, the drug release from the AGO solution was quick (90% over 2 h) due to rapid AGO release from the solution. The AGO release pattern from the optimized formulation was bi-phasic, with a limited initial burst release for only two hours and a durable sustained release of five hours. The extended-release from the produced NLC was visible in the optimized NLC. According to data for NLCs, the position of the drug within the lipid matrix may be associated with the biphasic release pattern of the drug from the lipid matrix. Because of the lipid's quick cooling during the formation of the NLCs, the drug is more likely to be enriched in the outermost layers of the particles, which causes superficial trapping and, as a result, drug release. Additionally, the outer phospholipid layer of the NLCs can partially erode, causing the quick diffusion of the drug present in the hydrophobic layer. The correlation coefficient (r^2) value served as a measure for finding the release kinetic model which would better fit the release data. The release data from AGO-NLC followed the Korsmeyer-Peppas release kinetics model having r^2 = 0.9932 with n = 0.8245 suggesting anomalous or non-Fickian diffusion (Figure 7), which is related to both the diffusion of the drug and dissolution of the NLC matrix.

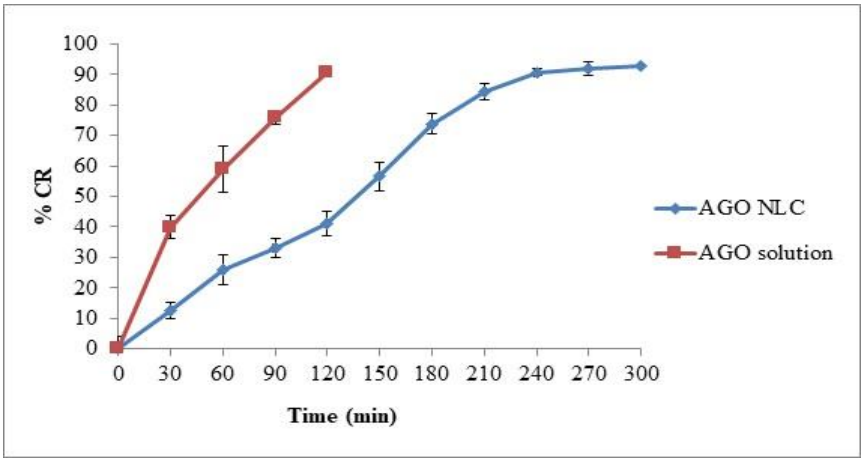

Figure 6. A comparative in vitro drug release profile of AGO solution and AGO-loaded NLC; mean ± SD, n=3

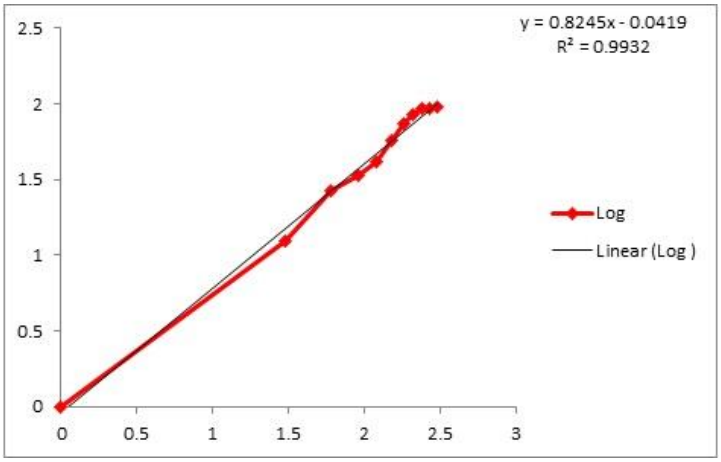

Figure 7. Korsmeyer-Peppas release kinetics model

2.3.9. Ex-vivo diffusion study of optimized AGO–loaded NLCs

AGO-loaded NLC exhibited significantly improved permeation (in comparison to AGO solution), according to the data from the permeation investigations of AGO solution and optimized AGO-loaded NLC using sheep nasal mucosa. At the same time period (5 h), 92.35% of AGO was penetrated from the optimized NLC formulation, compared to the 37% of AGO solution (Figure 8). AGO in NLC has much better penetration across the nasal mucosa due to its relatively increased lipophilicity [31].

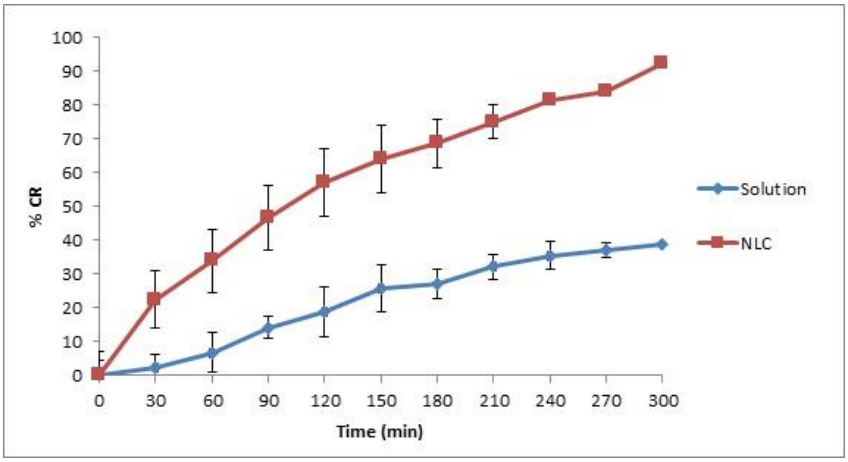

Figure 8. A comparative ex-vivo drug permeation profile of AGO solution and AGO-loaded NLC; mean ± SD, n=3

2.3.10. Nasal ciliotoxicity studies

Ciliotoxicity experiments were carried out to evaluate the toxicity of the specified excipients used in the preparation of AGO-loaded NLCs. The gathered visuals showed that tissue samples exposed to the positive control - Isopropyl alcohol (IPA) had a substantial negative influence on the sample, causing nasal mucosa injury, mucosal shrinking, and elimination of both cilia and epithelial cells. On the other hand, Negative-controlled – Phosphate buffer solution (PBS) samples displayed healthy epithelial layers and unharmed nasal cilia cells. However, there was no negative impact observed in the nasal mucosa samples treated with optimized AGO-loaded NLC (Figure 9). The nasal ciliotoxicity experiments confirmed that each excipient used in the formulation of AGO-loaded NLC was suitable to be administered through the nose [32].

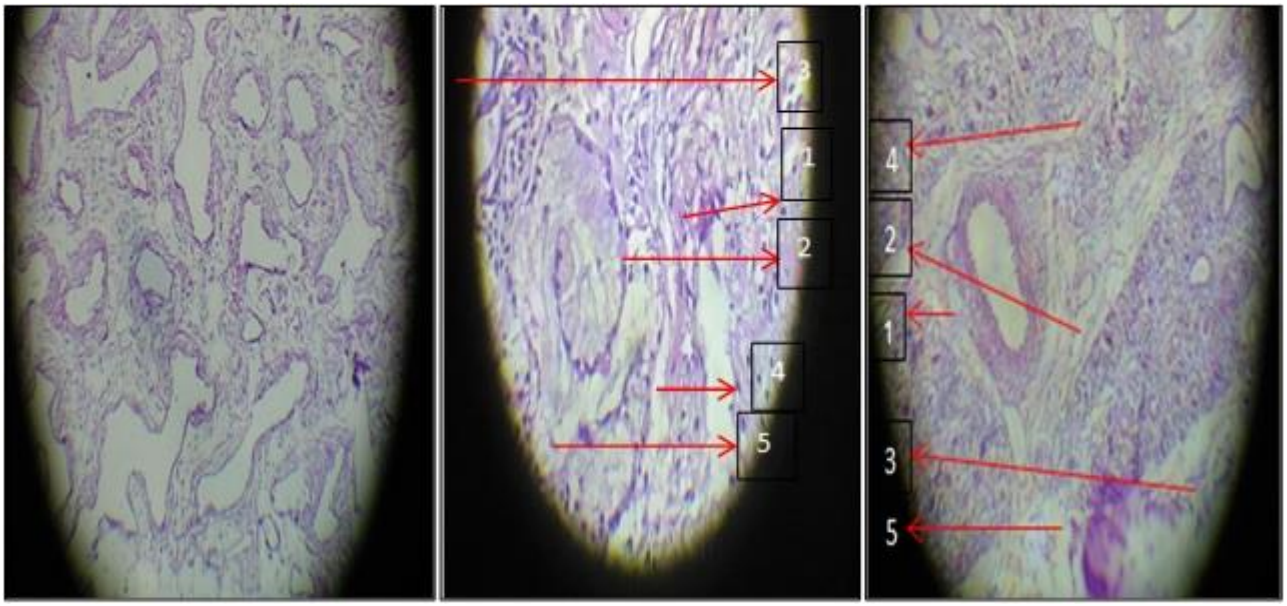

Figure 9. Histopathological sections of sheep nasal mucosa treated with a) IPA B) AGO-loaded NLC and c) PBS for nasal ciliotoxicity studies (1. Olfactory glands 2. Lamina Propria 3. Respiratory epithelium 4. Nuclei of Supportive cell 5. Goblet Cells)

2.3.11. Stability Study

Optimized NLC formulation was subjected to the stability analysis for 0, 30, 60, and 90 days, during that time changes in particle size, zeta potential, and entrapment efficiency were noted and estimated as indicated in Table 6. There was no physical change appeared in the formulation during this time period. The particle size of AGO-loaded NLCs remained stable at 0, 30, 60, and 90 days, and any slight increments in particle size could be attributed to particle aggregation or cohesion. While there was no substantial alteration observed in the zeta potential and entrapment efficiency within the 0 to 90-day timeframe. Therefore, based on the obtained data, it is evident that the formulation did not undergo any physical or chemical changes, demonstrating the stability of the prepared AGO-loaded NLCs formulation.

Table 6. Stability study of optimized AGO-loaded NLC formulation

Months	Particle size (nm)	Zeta potential (mV)	Entrapment efficiency (%)
0	122 ± 3.19	-33 ± 2.35	90.57 ± 0.987
1	131 ± 2.23	-32 ± 2.12	90.5 ± 0.9
2	135 ± 3.37	-33 ± 2.75	90 ± 1.1
3	135 ± 3.64	-33 ± 2.63	90.4 ± 0.7

Each value represents mean ± SD (n=3)

3. CONCLUSION

The developed and optimized AGO-loaded NLCs for the treatment of depression have become evident in the current investigation. The melt emulsification process, which included ultrasonication, was found to be successful in producing the drug-loaded NLCs. Box-Behnken design and Response surface approach were used for experimental design and optimization respectively. The optimized formulation showed a particle size of 122 nm, which was as expected to increase the cell penetration upon intranasal administration and was within the permissible particle size range for brain delivery. In addition, we have discovered a greater drug release profile (sustained release for 5 h up to 94% after the initial burst) and superior entrapment efficiency (90.57%). The Korsmeyer-Peppas release kinetics model was the one that best fit the Agomelatine release data, showing anomalous or non-fickian diffusion that is connected to both the drug's diffusion and the NLC matrix's dissolution. TEM study confirmed the spherical shape and homogeneity of NLCs. Although, the FTIR study provided that there was no interaction proceeded in between drug and excipients. In conclusion, the goals of this research were achieved i.e. to develop more affordable, biodegradable, sustainable nanocarriers with a higher drug entrapment and prolonged release profile.

4. MATERIALS AND METHODS

4.1. Materials

Agomelatine API was received as a gift sample from Mehta API Pvt. Ltd. Mumbai. Neroli oil was purchased from Deve Herbs. Furthermore, Glyceryl monostearate and Tween 80 were received as a free gift from Mohini Organics Pvt. Ltd. Mumbai. Poloxamer 188 was provided as a gift sample by BASF India Ltd. All the other additives utilized throughout the investigation were of analytical grade.

4.2. Methods

4.2.1. Screening of lipids

Determination of solid lipid was carried out by screening various solid lipids including GMS, Compritol® 888ATO, stearic acid, Gelucire 43/01, and Precirol® ATO 5. Briefly, the temperature of each solid lipid was raised by 5°C above its melting point, and after that AGO was introduced into the molten lipid. It's important to note that the proportion of AGO and solid lipid remains constant adhering to 1:1. Solid lipid which exhibited the most solubility of AGO was visibly evaluated and preferred for further study [35].

Different liquid lipids such as castor oil, oleic acid, isopropyl myristate, mono- and diglycerides, and Neroli oil, were screened in order to determine the best one. In a concise procedure, an accurately weighed quantity of the drug was slowly added into the 5 ml of liquid lipid while continuous stirring was maintained by a magnetic stirrer for 30 min after every addition. The point of saturation was identified by the loss of transparency. The resulting solution was then centrifuged (Beckman coulter, USA optima max- xp) at 50,000 rpm for 30 min. The supernatant was collected and analyzed by using high-pressure liquid chromatography HPLC (Agilent 1260 Quaternary HPLC) [36]. Chromatographic analysis was performed by using enable C18 G column and isocratic elution was carried out with a mobile phase consisting of acetonitrile: methanol: water (55:25:20) at a flow rate of 1.0 ml/min. Detection was carried out at 230 nm with a run time of 10 min. The mobile phase was freshly prepared and sonicated for 5 min to degas the solvent. The column and HPLC system were maintained at ambient temperature. The HPLC method was previously developed and validated by *Thota et al* [34].

4.2.2. Screening of surfactant

For screening of surfactant, transmittance % was measured using the method described by Alam et al. Briefly, a solution containing 5% surfactant was formulated. Simultaneously, in a distinct vessel, a predetermined quantity of a solid-liquid lipid blend (referred to as $lipid_{mix}$) was immersed in 3 ml of a volatile solvent, specifically methylene chloride, under consistent stirring. Subsequently, the $lipid_{mix}$ was introduced into the previously described surfactant solution in order to generate a colloidal system known as Nanostructured Lipid Carriers (NLC). Throughout this process, stirring was sustained to facilitate the evaporation of methylene chloride. The resultant solution was then subjected to analysis using a UV spectrophotometer (Shimadzu UV – 1800) at a wavelength of 650 nm [37].

4.2.3. Experiment design (Box-Behnken design)

Design Expert (version 8.0.7.1; M/s Stat-Ease, Minneapolis, USA) was utilized for designing the experiment. Formulation optimization of the prepared NLC was carried out by using response surface methodology, specifically the three-level, three-factor Box-Behnken design. The Box-Behnken design was discovered to be the most suitable design for analyzing quadratic response surfaces based on prior research and formulation variables, enabling optimization of the process with the least number of runs (13). Different independent and dependent variable values, as well as each variable's corresponding levels, were defined in Table 7.

Table 7. Defining different variables and their respective levels of Box-Behnken design for optimization of NLC

Variables	Levels		
Independent variables	-1	0	+1
Factor 1 = Total lipid %	1	2.5	4
Factor 2 = Surfactant concentration (%)	1	1.5	2
Factor 3 = Ultrasonication time (min)	5	7.5	10
Dependent variables	Constraints		
Response 1 = Particle size (nm)	Minimum		
Response 2 = Zeta potential (mV)	Maximize		
Response 3 = Entrapment Efficiency (%)	Maximize		

4.2.4. Preparation of AGO-loaded nanostructured lipid carrier

In order to formulate the NLCs (AGO-loaded nano lipid carriers), a melt emulsification-ultrasonication method was used [38, 39]. GMS and Neroli oil have been employed as the solid and liquid lipids for producing NLCs, respectively. The lipid phase was heated at a temperature above 10°C of melting of solid lipid. The aqueous phase was slowly added in the liquid phase while continuously stirring to get pre-emulsion. The obtained homogenated pre-emulsion was ultrasonicated for 5 min and cooled to get NLC [40].

4.2.5. Fourier Transform Infrared Spectroscopy (FTIR) study

FTIR spectroscopy was carried out to examine the potential interactions and compliance between the drug and the lipids utilized in NLC synthesis. FTIR instrument (Shimadzu IR Affinity-1) was used for conducting FTIR analysis of pure drug (AGO), drug in addition with lipids and surfactants. The scanning was conducted with Transmission mode in a wavenumber range of 4500 to 500 cm^{-1}.

4.2.6. Differential scanning calorimetry (DSC) study

Differential Scanning Calorimetry (DSC) (Mettler Toledo, USA) was used to analyze the thermal characteristics of pure drug AGO, the physical mixture of the drug and excipients, and optimized NLCs preparation. Accurately weighed samples were placed within a standard aluminum pan with a small perforation. The measurement started at a temperature of 30°C and ended at 300°C with a constant heating rate of 10°C/min and throughout this time period, the sample was continuously nitrogen purged at a flow rate of 40-60 ml/min. All samples were subjected to the same procedure.

4.2.7. Particle size analysis and PDI

Particle size analyzer (Zetasizer, Malvern, UK) with a dynamic light scattering technique was utilized to evaluate the particle size and PDI of the produced NLC formulations. The drug-loaded nanocarriers were examined at room temperature (25°C) after diluting them with double distilled water [41].

4.2.8. Zeta potential

The zeta potential or surface charge of the produced NLCs was determined by employing the zetasizer with electrophoretic light scattering technique. Evaluations were performed in a triplicate manner to obtain average zeta potential and standard deviation.

4.2.9. Entrapment efficiency %

It was calculated on the basis of the total amount of drug and free drug present in the sample (Eq. 4). The samples were placed in the 5 ml centrifugation tube and centrifuged (Beckman coulter, USA, OPTIMA MAX-XP) for 30 minutes at 50,000 rpm, and 4°C temperature. After collecting and filtering the supernatant, a UV spectrophotometer at a wavelength of 230 nm was used to determine the drug concentration. The subsequent equation was applied to calculate the entrapment efficiency.

$$\text{Entrapment Efficiency \%} = \left(\frac{\text{Total amount of drug} - \text{Amount of free drug}}{\text{Total amount of drug}}\right) \times 100 \quad \ldots\ldots\ldots\ldots\ldots (4)$$

4.2.10. Transmission Electron Microscopy (TEM)

Transmission electron microscopy was carried out using TEM (CM 200, Philips Briarcliff Manor, NY). The samples were diluted in double distilled water and subsequently subjected to negative staining using a 2% phosphotungstic acid solution. Afterward, they were allowed to air dry on a copper grid before undergoing analysis and analyzed at an accelerating voltage of 200 kV [42].

4.2.11. In-vitro drug release study

An in-vitro release analysis of the AGO from NLCs solution was carried out in phosphate buffer solution pH 6.8 employing a Franz Diffusion cell with a dialysis membrane. The molecular weight cut off of the dialysis membrane was about 14000 Da and the diffusion cell volume was 20 ml. The dialysis membranes were first immersed in phosphate buffer solution (PBS) pH 6.8 for overnight before conducting the study in order to saturate the membrane. PBS pH 6.8 was used to fill the diffusion cell, and a dialysis membrane was attached to the cell and the temperature was constantly held upon 37°C. A 30 minutes pre-incubation period was followed by the placement of the donor chamber with the AGO NLC formulation. A 3 ml sample from each batch was taken out of the receptor compartment at specified intervals during the study and analyzed at a wavelength of 230 nm by UV spectrophotometer.

4.2.12. Ex-vivo diffusion study of optimized AGO–loaded NLCs

Ex-vivo permeability study for AGO solution and drug-loaded NLCs was carried out using sheep nasal mucosa. A local butchery facility provided the sheep nasal mucosa, which was then washed with PBS. The collected nasal mucosa was cut into 2 cm^2 pieces with a thickness of 0.2 mm to be placed on the donor and receptor compartment of the diffusion cell. The volume of the diffusion cell used was 20 ml. Furthermore, the nasal mucosa was stabilized using PBS solution for about 15 minutes at a temperature of 37 ± 0.5 °C. The samples were placed in the donor compartment and collected after regular intervals and analyzed by UV spectrophotometer at a wavelength of 230 nm [43].

4.2.13. Nasal ciliotoxicity study

The nasal ciliotoxicity study has been performed utilizing freshly extracted sheep mucosa, and tissue samples were treated separately with PBS (negative control) and isopropyl alcohol (Positive control) and optimized NLCs formulation as a test after ex-vivo diffusion. The tissue samples were stained by hematoxylin and eosin and a histopathology study was carried out [44].

4.2.14. Stability study

The optimized NLC formulation was subjected to a stability study as per the International Council on Harmonization (ICH) guidelines (40 ± 2°C temperature and 75 ± 5% RH) for 0, 30, 60, and 90 days. In order to examine the stability various parameters were evaluated such as particle size, zeta potential, and entrapment efficiency.

Acknowledgements: The authors are really thankful to Mehta API Private Limited, Mumbai, India for providing a gift sample of agomelatine and Dr. Ashturkar's pathology lab for toxicity evaluation by screening nasal mucosa. The authors express their gratitude to BASF India Ltd. for providing a gift sample of the surfactants. Authors are also

grateful to Marathwada Mitra Mandal's College of Pharmacy Pune for providing facilities and continuous guidance throughout the research.

Author contributions: Concept – S.S., K.T.; Design – S.S., K.T., M.R., G.K.; Supervision – S.S., M.R.; Resources – S.S., K.T.; Materials – M.R..; Data Collection and/or Processing – K.T., G.K.; Analysis and/or Interpretation – S.S., K.T., M.R., G.K.; Literature Search – S.S., K.T.; Writing – S.S., K.T., G.K.; Critical Reviews – M.R., G.K.

Conflict of interest statement: "The authors declared no conflict of interest" in the manuscript.

Financial support: None

Ethics statement: None

REFERENCES

[1] Gong Q, He Y. Depression, neuroimaging and connectomics: A selective overview. Biol Psychiatry. 2015; 77(3): 223–235. https://doi.org/10.1016/j.biopsych.2014.08.009

[2] Vos T, Lim S, Abbafati C, Abbas K, Abbasi M, Abbasifard M, AbbasiKangevari M, Abbastabar H, Abd-Allah F, Abdelalim A. Global burden of 369 diseases and injuries in 204 countries and territories, 1990–2019: A systematic analysis for the Global Burden of Disease Study 2019. Lancet. 2020; 396(1204): 1222. https://doi.org/10.1016/S0140-6736(20)30925-9

[3] Kennedy SH, Guilleminault C. P.2.C.013 antidepressant efficacy of agomelatine 25-50 mg versus venlafaxine 75-150 mg: Two randomized, double blind studies. Eur Neuropsychopharmacol. 2006; 16. https://doi.org/10.1016/s0924-977x(06)70347-9

[4] Cascade E, Kalali AH, Kennedy SH. Real-World Data on SSRI Antidepressant Side Effects. Psychiatry (Edgmont). 2009;6(2):16-18.

[5] Marasine NR, Sankhi S, Lamichhane R, Marasini NR, Dangi NB. Use of antidepressants among patients diagnosed with depression: A scoping review. Biomed Res Int. 2021; 2021:6699028. https://doi.org/10.1155/2021/6699028

[6] De Berardis D, Fornaro M, Serroni N, Campanella D, Rapini G, Olivieri L, Srinivasan V, Lasevoli F, Tomasetti C, De Bartolomeis A, Valchera A, Perna G, Mazza M, Di Nicola M, Martinotti G, Di Giannantomio M. Agomelatine beyond borders: Current evidences of its efficacy in disorders other than major depression. Int J Mol Sci. 2015; 16(1): 1111–1130. https://doi.org/10.3390/ijms16011111

[7] Bourin M, Mocaer E, Porsolt R. Antidepressant-like activity of S 20098 (agomelatine) in the forced swimming test in rodents: Involvement of melatonin and serotonin receptors. J Psychiatry Neurosci. 2004; 29(2): 126-133.

[8] Loo H, Hale A, Dhaenen H. Determination of the dose of agomelatine, a melatoninergic agonist and selective 5-HT2C antagonist, in the treatment of major depressive disorder: A placebo-controlled dose range study. Int Clin Psychopharmacol. 2002; 17(5): 239–247. https://doi.org/10.1097/00004850-200209000-00004

[9] Guardiola-Lemaitre B, De Bodinat C, Delagrange P, Millan MJ, Munoz C, Mocaer E. Agomelatine: Mechanism of action and pharmacological profile in relation to antidepressant properties. Br J Pharmacol. 2014; 171(15): 3604–3619. https://doi.org/10.1111/bph.12720

[10] Gorwood P, Benichou J, Moore N, Wattez M, Secouard M-C, Desobry X, Picarel-Blanchot F, De Bodinat C. Agomelatine in standard medical practice in depressed patients: Results of a 1-year multicentre observational study in France. Clin Drug Investig. 2020; 40(11): 1009–1020. https://doi.org/10.1007/s40261-020-00957-9

[11] De Berardis D, Serroni N, Campanella D, Rapini G, Olivieri L, Feliziani B, Carano A, Valchera A, Lasevoli F, Tomasetti C, Mazza M, Fornaro M, Perna G, Di Nicola M, Martinotti G, Di Giannantonio M. Alexithymia, responsibility attitudes and suicide ideation among outpatients with obsessive-compulsive disorder: An exploratory study. Compr Psychiatry. 2015; 58: 82–87. https://doi.org/10.1016/j.comppsych.2014.12.016

[12] Kennedy SH, Rizvi SJ. Agomelatine in the treatment of major depressive disorder. CNS Drugs. 2010; 24(6): 479–499. https://doi.org/10.2165/11534420-000000000-00000

[13] Engelhardt B, Liebner S. Novel insights into the development and maintenance of the blood–brain barrier. Cell Tissue Res. 2014; 355(3): 687–699. https://doi.org/10.1007/s00441-014-1811-2

[14] Du W, Zhou Y, Gong Y, Zhao C. Investigation of physicochemical properties and in-vitro in-vivo evaluation of Agomelatine polymorphs. Asian J Pharm. 2013; 8(3): 181-190. https://doi.org/10.1016/j.ajps.2013.07.024

[15] Mahajan HS, Mahajan MS, Nerkar PP, Agrawal A. Nanoemulsion-based intranasal drug delivery system of saquinavir mesylate for brain targeting. Drug Deliv. 2013; 21(2): 148–154. https://doi.org/10.3109/10717544.2013.838014

[16] Gadhave D, Choudhury H, Kokare C. Neutropenia and leukopenia protective intranasal olanzapine-loaded lipid-based nanocarriers engineered for brain delivery. Appl Nanosci. 2018; 9(2): 151–168. https://doi.org/10.1007/s13204-018-0909-3

[17] Gorain B, Rajeswary DC, Pandey M, Kesharwani P, Kumbhar SA, Choudhury H. Nose to brain delivery of nanocarriers towards attenuation of demented condition. Curr Pharm Des. 2020; 26(19): 2233–2246. https://doi.org/10.2174/1381612826666200313125613

[18] Md S, Gan SY, Haw YH, Ho CL, Wong S, Choudhury H. In vitro neuroprotective effects of naringenin nanoemulsion against β-amyloid toxicity through the regulation of amyloidogenesis and tau phosphorylation. Int J Biol Macromol. 2018; 118: 1211–1219. https://doi.org/10.1016/j.ijbiomac.2018.06.190

[19] Micheli M-R, Bova R, Magini A, Polidoro M, Emiliani C. Lipid-based nanocarriers for CNS-targeted drug delivery. Recent Pat CNS Drug Discov. 2012; 7(1): 71–86. https://doi.org/10.2174/157488912798842241

[20] Sapra B, Thatai P, Bhandari S, Sood J, Jindal M, Tiwary A. A critical appraisal of microemulsions for drug delivery: Part I. Ther Deliv. 2013; 4(12): 1547–1564. https://doi.org/10.4155/tde.13.116

[21] Choudhury H, Gorain B, Karmakar S, Biswas E, Dey G, Barik R, Mandal M, Pal TK. Improvement of cellular uptake, in vitro antitumor activity and sustained release profile with increased bioavailability from a nanoemulsion platform. Int J Pharm. 2014; 460(1–2): 131–143. https://doi.org/10.1016/j.ijpharm.2013.10.055

[22] Choudhury H, Pandey M, Chin PX, Phang YL, Cheah JY, Ooi SC, Mak KK, Pichika MR, Kesharwani P, Hussain Z, Gorain B. Transferrin receptors-targeting nanocarriers for efficient targeted delivery and transcytosis of drugs into the brain tumors: A review of recent advancements and emerging trends. Drug Deliv Transl Res. 2018; 8(5): 1545–1563. https://doi.org/10.1007/s13346-018-0552-2

[23] Cunha S, Amaral MH, Lobo JM, Silva AC. Lipid nanoparticles for nasal/intranasal drug delivery. Crit Rev Ther Drug Carr Syst. 2017; 34(3): 257–282. https://doi.org/10.1615/critrevtherdrugcarriersyst.2017018693

[24] Fachel FNS, Nemitz MC, Medeiros-Neves B, Veras KS, Bassani VL, Koester LS, Henriques AT, Teixeira HF. A novel, simplified and stability-indicating high-throughput ultra-fast liquid chromatography method for the determination of rosmarinic acid in nanoemulsions, porcine skin and nasal mucosa. J Chromatogr B. 2018; 1083: 233–241. https://doi.org/10.1016/j.jchromb.2018.03.020

[25] Garces A, Amaral MH, Sousa Lobo JM, Silva AC. Formulations based on solid lipid nanoparticles (SLN) and nanostructured lipid carriers (NLC) for cutaneous use: A Review. Eur J Pharm Sci. 2018; 112: 159–167. https://doi.org/10.1016/j.ejps.2017.11.023

[26] Zheng M, Falkeborg M, Zheng Y, Yang T, Xu X. Formulation and characterization of nanostructured lipid carriers containing a mixed lipids core. Colloids Surf A: Physicochem Eng Asp. 2013; 430: 76–84. https://doi.org/10.1016/j.colsurfa.2013.03.070

[27] Cirri M, Bragagni M, Mennini N, Mura P. Development of a new delivery system consisting in "Drug – in Cyclodextrin – in nanostructured lipid carriers" for ketoprofen topical delivery. Eur J Pharm Biopharm. 2012; 80(1): 46–53. https://doi.org/10.1016/j.ejpb.2011.07.015

[28] Souto EB, Baldim I, Oliveira WP, Rao R, Yadav N, Gama FM, Mahant S. SLN and NLC for topical, dermal, and transdermal drug delivery. Expert Opin Drug Deliv. 2020; 17(3): 357–377. https://doi.org/10.1080/17425247.2020.1727883

[29] Zheng M, Falkeborg M, Zheng Y, Yang T, Xu X. Formulation and characterization of nanostructured lipid carriers containing a mixed lipids core. Colloids Surf A: Physicochem. Eng. 2013; 430: 76–84. https://doi.org/10.1016/j.colsurfa.2013.03.070

[30] Shukla T, Upmanyu N, Pandey SP, Gosh D. Chapter 1 – Lipid nanocarriers. Lipid Nanocarriers for Drug Targeting, 2018; 1–47. https://doi.org/10.1016/b978-0-12-813687-4.00001-3

[31] Khan A, Imam SS, Aqil M, Ahad A, Sultana Y, Ali A, Khan K. Brain targeting of temozolomide via the intranasal route using lipid-based nanoparticles: Brain Pharmacokinetic and scintigraphic analyses. Mol Pharmaceutics. 2016; 13(11): 3773–3782. https://doi.org/10.1021/acs.molpharmaceut.6b00586

[32] Madane RG, Mahajan HS. Curcumin-loaded nanostructured lipid carriers (NLCs) for nasal administration: Design, characterization, and in vivo study. Drug Deliv. 2016; 23(4): 1326–1334. https://doi.org/10.3109/10717544.2014.975382

[33] Graeser, KA, Patterson JE, Zeitler JA, Rades T. The role of configurational entropy in amorphous systems. Pharmaceutics. 2010; 2: 224–244.

[34] Meghana M, Thota S, Venisetty RK. Development and validation of stability- indicating RP-HPLC method for the estimation of Agomelatine in API. Res J Pharm Biol Chem Sci. 2014; 5(1): 621-628.

[35] Alam M, Ahmed S, Nikita, Moon G, Aqil Mohd, Sultana Y. Chemical engineering of a lipid nano-scaffold for the solubility enhancement of an antihyperlipidaemic drug, simvastatin; Preparation, optimization, physicochemical characterization and pharmacodynamic study. Artif Cells Nanomed Biotechnol. 2018; 1908-1919. https://doi.org/10.1080/21691401.2017.1396223

[36] Gadhave DG, Kokare CR. Nanostructured lipid carriers engineered for intranasal delivery of teriflunomide in multiple sclerosis: Optimization and in vivo studies. Drug Dev Ind Pharm. 2019; 45(5): 839–851. https://doi.org/10.1080/03639045.2019.1576724

[37] Pokharkar V, Patil-Gadhe A, Palla P. Efavirenz loaded nanostructured lipid carrier engineered for brain targeting through intranasal route: In-vivo pharmacokinetic and toxicity study. Biomed Pharmacother. 2017; 94: 150–164. https://doi.org/10.1016/j.biopha.2017.07.067

[38] Kawish SM, Ahmed S, Gull A, Aslam M, Pandit J, Aqil M, Sultana Y. Development of nabumetone loaded lipid nano-scaffold for the effective oral delivery; optimization, characterization, drug release and pharmacodynamic study. J Mol Liq. 2017; 231: 514–522. https://doi.org/10.1016/j.molliq.2017.01.107

[39] Iqbal R, Ahmed S, Jain GK, Vohora D. Design and development of letrozole nanoemulsion: A comparative evaluation of brain targeted nanoemulsion with free letrozole against status epilepticus and neurodegeneration in mice. Int J Pharm. 2019; 565: 20–32. https://doi.org/10.1016/j.ijpharm.2019.04.076

[40] Mahmood S, Mandal UK, Chatterjee B. Transdermal delivery of raloxifene HCl via ethosomal system: Formulation, advanced characterizations and pharmacokinetic evaluation. Int J Pharm. 2018; 542(1–2): 36–46. https://doi.org/10.1016/j.ijpharm.2018.02.044

[41] Galgatte UC, Kumbhar AB, Chaudhari PD. Development of institute for nasal delivery: Design, optimization, in vitro and in vivo evaluation. Drug Deliv. 2014; 21(1): 62–73. https://doi.org/10.3109/10717544.2013.849778

[42] Sood S, Jain K, Gowthamarajan K. Optimization of curcumin nanoemulsion for intranasal delivery using design of experiment and its toxicity assessment. Colloids Surf B. 2014; 113: 330–337. https://doi.org/10.1016/j.colsurfb.2013.09.030

[43] Kumar P, Sharma G, Kumar R, Singh B, Malik R, Katare OP, Raza K. Promises of a biocompatible nanocarrier in improved brain delivery of quercetin: Biochemical, pharmacokinetic and biodistribution evidences. Int J Pharm. 2016; 515(1–2): 307–314. https://doi.org/10.1016/j.ijpharm.2016.10.024

[44] Anand A, Arya M, Kaithwas G, Singh G, Saraf SA. Sucrose stearate as a biosurfactant for development of rivastigmine containing nanostructured lipid carriers and assessment of its activity against dementia in C. elegans model. J Drug Deliver Sci Technol. 2019; 49: 219–226. https://doi.org/10.1016/j.jddst.2018.11.021